Available online at www.sciencedirect.com
SCIENCE DIRECT®
Journal of Chromatography A, 1064 (2005) 25–38
JOURNAL OF CHROMATOGRAPHY A
www.elsevier.com/locate/chroma

New hybrid polymeric liquid chromatography chiral stationary phase prepared by surface-initiated polymerization

F. Gasparrini*, D. Misiti, R. Rompietti, C. Villani

Dipartimento di Studi di Chimica e Tecnologia delle Sostanze Biologicamente Attive, Università degli Studi di Roma "La Sapienza", P.le A. Moro 5, 00185 Roma, Italy

Received 6 October 2004; received in revised form 22 November 2004; accepted 24 November 2004
Available online 24 December 2004

Abstract

A new hybrid organic/inorganic HPLC chiral stationary phase (CSP1) has been synthesized by the *grafting from* (*g-from*) radical polymerization of an enantiopure diacryloyl derivative of *trans*-1,2-diaminocyclohexane in the presence of mesoporous, azo-activated silica particles. The new chiral stationary phase has been fully characterized by elemental analysis, differential scanning calorimetry, diffuse reflectance infrared spectroscopy, scanning electron microscopy, inverse size exclusion chromatography and Van Deemter analysis. CSP1 shows improved chromatographic performances compared to its analog CSP2 synthesized by the alternative *grafting to* (*g-to*) approach in which the azo initiator is kept in solution. CSP1 can successfully resolve several chemically diverse chiral compounds, using both organic and water-based eluents (normal phase, polar organic, etc.).

Keywords: HPLC; Enantioselectivity; Chiral stationary phase; Chiral polymer; Hybrid-CSP

1. Introduction

In recent years, the chromatographic separation of enantiomers on chiral stationary phases (CSPs) has emerged as one of the most efficient technique applicable from the analytical to the preparative scale [1–3].

CSPs for high-performance liquid chromatography (HPLC) can be divided in two classes according to the molecular size of the chiral selector they contain: brush-type CSPs based on low-molecular mass selectors [4] and polymeric CSPs having large macromolecular selectors like proteins [5], polysaccharides and their derivatives [6], synthetic polymers [7].

CSPs, containing surface-adsorbed polysaccharides derivatives, especially cellulose and amylose carbamates, are extensively used at analytical and preparative levels as they can resolve the enantiomers of a wide range of chiral compounds [8].

However, research on CSPs based on totally synthetic, surface-linked optically active polymers is also rapidly evolving. Attractive features of these types of CSPs are the large chemical and structural variability that can be exploited in the preparation of the chiral selectors, the possibility of having the two enantiomeric versions of the CSP, and the chemical and thermal inertness of the packing material that derives from the covalent attachment of the chiral polymer to the solid support. However, CSPs based on chiral polymers covalently linked to an HPLC silica matrix, may suffer from slow analyte mass transfer kinetics and reduced efficiency if the degree of polymerization, grafting density and polymer architecture are not properly controlled. Polymeric materials forming a thin, ordered layer on the silica surface without altering the pores morphology, are therefore, highly desirable for the preparation of improved polymeric CSPs.

Several strategies are available for the preparation of uniform, polymeric materials for non-chromatographic applications, where a polymer layer is end-grafted to flat or porous surfaces like gold, silicon or silica [9,10]. Achiral polymer brushes linked to silica particles that are effective in

* Corresponding author. Tel.: +39 06 499 12776; fax: +39 06 499 12780.
E-mail address: francesco.gasparrini@uniroma1.it (F. Gasparrini).

0021-9673/$ – see front matter © 2004 Elsevier B.V. All rights reserved.
doi:10.1016/j.chroma.2004.11.089

reversed phase HPLC separations have also been described [11].

Here, we describe a procedure for the generation of a new hybrid silica/chiral polymeric material (CSP1) using a radical polymerization process that begins directly from the surface of azo-activated silica particles and employs the *N*,*N*′-diacryloyl derivative of (*R*,*R*)-1,2-diaminocyclohexane as chiral monomer. To the best of our knowledge, it is the first example of the application of the *g-from* approach to the synthesis of a chiral stationary phase for HPLC applications.

The complete physico-chemical and chromatographic characterizations of CSP1 are reported. In addition, a comparison with the related CSP2 prepared by the alternative approach (*g-to*) in which the azo initiator is kept in solution is presented.

2. Experimental

2.1. Apparatus

Analytical liquid chromatography was performed on a Waters chromatograph equipped with a Rheodyne model 7725i 20 μL loop injector (200 μL loop for the loading studies), a 1525 binary HPLC pump, a dual wavelength absorbance detector, and a Jasco Mod 995-CD detector. Chromatographic data were collected and processed using Empower software (Waters, Milford, MA, USA). DRIFT and transmission IR (potassium bromide pellets or liquid paraffin dispersion) spectra were recorded on a Jasco 430 Fourier transform (FT) IR spectrometer (Jasco Europe, Italy) at a resolution of 4 cm^{-1}. NMR spectra were recorded on a Bruker Avance 400 spectrometer. Melting points were determined on a Büchi B-545 instrument (Flawil, Switzerland). Optical rotation values were obtained on a Jasco P1030 polarimeter (Jasco Europe, Italy). DSC traces were recorded on a Mettler Toledo STARe System (Columbus, OH, USA) at a scan rate of 10 °C min^{-1}. Scanning electron microscopy was performed on a LEO1450VP instrument; samples were gold-sputtered to reduce charge effects.

2.2. Reagents

Spherical Daisogel SP-300-5P (5 μm particle size, 115 m^2 g^{-1}) silica gel was purchased from Daiso (Japan). Spherical Kromasil Si-100 (5 μm particle size, 340 m^2 g^{-1}) and spherical Kromasil Si-200 (5 μm particle size, 213 m^2 g^{-1}) were purchased from Eka Chemicals (Sweden). (1*R*,2*R*)-diaminocyclohexane, diisopropylethylamine, acryloyl chloride, 3-aminopropiltrietoxysilane, vinyltriacetoxysilane, phosphorous pentachloride, naphthalene, biphenyl, nitrobenzene, 1,3-dinitrobenzene, *N*-aminoacid derivatives, 1,1′-bi-2-naphthol, dry toluene and hydrogen fluoride pyridine solution (∼70% HF) were purchased from Fluka (Sigma–Aldrich Company, Buchs, Switzerland); 4,4′-azobis-4-cyanopentanoic acid, *p*-terphenyl, anthracene, methyl benzoate, acetophenone and warfarin were purchased from Aldrich (Sigma–Aldrich Company, Buchs, Switzerdand); 1-methoxy-2-methyl-1-(trimethylsyliloxy)-1-propene was purchased from Lancaster (Clariant group, UK); ammonium acetate was purchased from T.J. Baker (Division of Mallinckrodt Baker Inc., Phillipsburg, NJ). HPLC-grade solvents were purchased from Merck (Darmstadt, Germany). Narrow molecular weight poly(styrene) standards were supplied from Waters (Milford, MA). Other chiral solutes were available from previous studies. Chloroform was dried by filtration through an open glass column filled with neutral alumina under inert atmosphere and then degassed with helium.

2.3. Preparation of N-(2-acryloylamino-(1R,2R)-cyclohexyl)-acrylamide (DACH-ACR)

To a solution of (1*R*,2*R*)-diaminocyclohexane (4.0 g, 35.03 mmol) in 50 mL of an anhydrous chloroform/toluene (2.5/1, v/v) mixture is added 12.0 mL of diisopropylethylamine (70.06 mmol). To the cooled (0 °C, ice bath) solution, is added dropwise over a period of 1.5 h, with magnetic stirring under an argon atmosphere, a solution of acryloyl chloride (5, 7 mL; 70.06 mmol) in 100 mL of an anhydrous chloroform/toluene (2.5/1, v/v) mixture. The reaction mixture is kept at 0 °C for 35 min, with magnetic stirring under an argon atmosphere. The white precipitate that forms is collected by filtration, washed with toluene and hexane and dried at reduced pressure (0.1 mbar, 25 °C) to yield 6.34 g of the title compound (82% yield). TLC: Merck plates Si-60-F_{254} eluent CH_2Cl_2/MeOH 90/10, R_f = 0.41. Elemental analysis: found %C, 63.31; %H, 7.99; %N, 12.06; calculated for $C_{12}H_{18}N_2O_2$ %C, 64.83; %H, 8.16; %N, 12.61. Mp: 233 °C. $[\alpha]_D^{20}$ = +85.4 (*c* = 1.0; DMSO). ^{1}H NMR ($^2H_6$DMSO) *δ*: 1.20–1.30 (m, 4H), 1.60–1.70 (m, 2H), 1.85–1.95 (m, 2H), 3.60–3.70 (m, 2H), 5.52 (dd, *J* = 9.90 Hz, 2.44 Hz, 2H), 6.02 (dd, *J* = 17.09 Hz, 2.44 Hz, 2H), 6.15 (dd, *J* = 17.09 Hz, 9.90 Hz, 2H), 7.85 (d, 2H). ^{13}C NMR ($^2H_6$DMSO) *δ*: 23.93, 31.30, 52.24, 124.74, 130.28, 166.14. FT-IR (KBr): 3284, 3075, 3033, 1656, 1625, 1550, 1410 cm^{-1}.

2.4. Preparation of the dichloride of 4,4′-azobis-4-cyanopentanoic acid [12]

Phosphorous pentachloride (8.0 g; 38.4 mmol) is dispersed in 40 mL of anhydrous CH_2Cl_2 (dispersion A). 4,4′-Azobis-4-cyanopentanoic acid (2.0 g; 9.6 mmol) is dispersed in 55 mL of anhydrous CH_2Cl_2 (dispersion B). Dispersion A is placed in a three necked round bottom flask equipped with addition funnel and magnetic stir bar and cooled to 0 °C with an ice bath. Dispersion B is then added dropwise over a 1 h period with continuous stirring under an argon atmosphere. The cooling bath is removed and stirring is continued at 20 °C for 6 h. Solid materials formed during the reaction or left over by reagents are removed by filtration, and the solution is concentrated to about 20 mL by evaporation at reduced pressure

(rotary evaporator, 250 mbar). Solid material formed upon concentration is removed by filtration. To the remaining solution is added hexane (20 mL) and the solution is kept at 4 °C for 12 h, under an argon atmosphere. The solid material that precipitates is isolated by suction filtration and dried at reduced pressure (0.1 mbar, 25 °C) to yield 1.80 g (77%) of the title compound. ^{1}H NMR (C^2HCl_3) δ: 1.69 (s, 3H), 1.75 (s, 3H), 2.43-2.54 (m, 2H), 2.56-2.64 (m, 2H), 2.92-3.08 (m, 2H), 3.11-3.22 (m, 2H). ^{13}C NMR (C^2HCl_3) δ: 23.75, 23.90, 33.04, 41.82, 41.92, 71.42, 71.57, 116.90, 117.00, 172.24, 172.32. FT-IR (Nujol): 2240, 1789, 1462 cm^{-1}.

2.5. Preparation of 3-aminopropyl silica gel (3-APSG)

Silica Daisogel SP-300-5P (10.0 g) (particle size 5 mμ; surface area 115 $m^2\,g^{-1}$; pore diameter 300 Å, pore volume 0.93 mL g^{-1}) is dried at reduced pressure (0.1 mbar) at 150 °C for 2 h (weight loss 2.5%). Dried silica is placed in a 500 mL three-necked round bottom flask equipped with a Dean Stark trap, reflux condenser and inert gas inlet, and 240 mL of toluene are added. The slurry is heated to reflux temperature (∼110 °C) with mechanical stirring under an argon atmosphere, and 25 mL of distillate are collected over a 1 h period. After cooling to room temperature, 5.0 mL of 3-aminopropyl-triethoxysilane (21.5 mmol) are added at once and the slurry is heated to reflux temperature for 4 h, with mechanical stirring under an argon atmosphere. After cooling to room temperature, modified silica is collected by filtration and washed with 200 mL portions of toluene, methanol, CH_2Cl_2 and dried at reduced pressure (0.1 mbar, T = 60 °C) up to constant weight (10.4 g; weight increment: 4.0%). Elemental analysis: %C, 1.35; %H, 0.54; %N, 0.48; 375 μmoles g^{-1}. FT-IR (DRIFT): 3432, 2978, 2935, 1874, 1630, 1095, 954, 802 cm^{-1}.

The following values from elemental analysis were obtained using Kromasil Si-200: %C, 2.31; %H, 0.96; %N, 0.83; 641 μmoles g^{-1}; and Kromasil Si-100: %C, 2.75; %H, 0.83; %N, 0.94; 764 μmoles g^{-1}.

2.6. Activation of 3-aminopropyl silica gel with the dichloride of 4,4′-azobis-4-cyanopentanoic acid (3-APSG-AZO)

Aminopropyl silica gel (3.0 g) is dispersed in 25 mL of anhydrous toluene with mechanical stirring and under an argon atmosphere. To the cooled (0 °C, ice bath) slurry is added dropwise a solution of 1-methoxy-2-methyl-1-(trimethylsyliloxy)-1-propene (500 μl; 2.45 mmol) in 5 mL of anhydrous toluene followed by a solution of the dichloride of 4,4′-azobis-4-cyanopentanoic acid in anhydrous toluene (336 mg; 1.22 mmol in 10 mL). The ice bath is removed and stirring is continued at 25 °C for 3 h. Modified silica is then isolated by filtration, washed with 100 mL portions of acetone, methanol, acetone, CH_2Cl_2 and dried at reduced pressure (0.1 mbar, T = 25 °C) (3.1 g; weight increment: 3.5%.) Elemental analysis: %C, 3.70; %H, 0.78; %N, 1.21; 279 μmoles g^{-1}. DSC: T_{dec} = 120 °C; I_{dec} = 44.77 J g^{-1}. FT-IR (DRIFT): 2978, 2941, 2898, 2244, 1649, 1548, 1446 cm^{-1}.

The following values from elemental analysis were obtained using Kromasil Si-200: %C, 6.20; %H, 1.24; %N, 2.13; 478 μmoles g^{-1}; and Kromasil Si-100: %C, 8.64; %H, 1.67; %N, 2.35; 486 μmoles g^{-1}.

2.7. One-step activation of 3-aminopropyl silica gel with 4,4′-azobis-4-cyanopentanoic acid and EEDQ (3-APSG-AZO) [13]

4,4′-Azobis-4-cyanopentanoic acid (1.0 g, 3.6 mmol) is dissolved in 30 mL of anhydrous *N*,*N*-dimethylformamide (DMF), with mechanical stirring and under inert atmosphere at room temperature. To the stirred solution is added 2-ethoxy-1-ethoxycarbonyl-1,2-dihydroquinoline (EEDQ, 1.78 g, 7.2 mmol) and, after complete dissolution, 3.0 g of 3-aminopropyl silica gel. The mixture is then kept at room temperature with continuous stirring and under inert atmosphere for 16 h. The modified silica gel (3-APSG-AZO) is collected by filtration, washed with successive 100 mL portions of DMF, methanol, dichloromethane and dried under reduced pressure (0.1 mbar) at room temperature to constant weight (3.1 g; weight increment: 3.5%). Elemental analysis: %C, 3.70; %H, 0.78; %N, 1.21; 279 μmoles g^{-1}. DSC: T_{dec} = 120 °C; I_{dec} = 44.77 J g^{-1}. FT-IR (DRIFT): 2978, 2941, 2898, 2244, 1649, 1548, 1446 cm^{-1}.

2.8. Preparation of CSP1 [14]

To a heated (60 °C) solution of *N*-(2-acryloylamino-(1*R*,2*R*)-cyclohexyl)-acrylamide in anhydrous, degassed $CHCl_3$ (450 mg in 50 mL) is added 3.0 g of 3-APSG-AZO with mechanical stirring and under an argon atmosphere. The slurry is heated with stirring at 60 °C for 5 h and then heated at reflux temperature for 1 h. After cooling to room temperature, modified silica is isolated by filtration, washed with 100 mL portions of methanol, acetone, CH_2Cl_2 and dried at reduced pressure (0.1 mbar, T = 60 °C) (3.4 g; weight increment: 12%). Elemental analysis: %C, 10.36; %H, 1.68; %N, 2.19; 392 μmoles g^{-1}. FT-IR (DRIFT): 3078, 2941, 2860, 2237, 1646, 1542, 1451 cm^{-1}.

The following values from elemental analysis were obtained using Kromasil Si-200: %C, 12.87; %H, 2.06; %N, 2.92; 393 μmoles g^{-1}; and Kromasil Si-100: %C, 14.88; %H, 2.53; %N, 2.99; 393 μmoles g^{-1}.

2.9. Dissolution of the CSP1 silica matrix by HF treatment

An hydrogen fluoride pyridine solution (∼70% HF, 2 mL) is cooled to 0 °C in an ice bath, with magnetic stirring. CSP1 (100 mg) is then added in a single portion and stirring is continued at 0 °C for 1 h and at 25 °C for additional 3 h.

The mixture is then centrifuged at 2000 rpm, the liquid phase is discarded and the remaining solid is washed several times with methanol and finally dried at reduced pressure. The amount of recovered material (amount ∼15 mg) is consistent with a complete destruction of the silica matrix. FT-IR (KBr): 3078, 2941, 2860, 2237, 1646, 1542, 1451 cm^{-1}.

2.10. Vinyl silica gel (VSG)

Silica Daisogel SP-300-5P (3.2 g) is dried at reduced pressure (0.1 mbar) at 150 °C for 2 h (weight loss 2.5%). Dried silica (3.013 g) is dispersed in 30 mL of toluene in a 100 mL three necked round bottom flask equipped with a Dean Stark trap, reflux condenser and inert gas inlet, and 2.04 mL of vinyltriacetoxysilane are added. The slurry is heated to reflux temperature (∼110 °C) with mechanical stirring under an argon atmosphere for 5 h. After cooling to room temperature, modified silica is collected by filtration and washed with 100 mL portions of toluene, methanol, CH_2Cl_2 and dried at reduced pressure (0.1 mbar, $T = 60$ °C) up to constant weight (3.074 g; weight increment: 2.0%). Elemental analysis: %C, 1.14; %H, 0. 42; 475 μmoles g^{-1}. FT-IR (DRIFT): 3069, 3028, 2992, 2964, 2851, 1876, 1726, 1604, 1412, 1090, 797 cm^{-1}.

2.11. Preparation of CSP2 [15]

VSG (3.042 g) is dispersed in a solution of DACH-ACR in anhydrous, degassed chloroform (0.450 g in 50 mL). The reaction mixture is heated to gentle reflux and a solution of AIBN in chloroform (0.045 g in 2 mL) is added via syringe, with mechanical stirring and under an argon atmosphere. The mixture is then kept at reflux temperature for 8 h. After cooling to room temperature, modified silica is collected by filtration and washed with 200 mL portions of $CHCl_3$, methanol, CH_2Cl_2 and dried at reduced pressure (0.1 mbar, $T = 60$ °C) up to constant weight (3.280 g; weight increment: 8.0%). Elemental analysis: %C, 6.82; %H, 1.08; %N, 1.13; 401 μmoles g^{-1}. FT-IR (DRIFT): 3077, 2939, 2862, 1872, 1639, 1543, 1452, 1087, 805 cm^{-1}.

2.12. Chromatographic procedures

The analytical stainless-steel columns (250 mm × 4.6 mm, $L \times$ i.d.), supplied by Alltech (Illinois, USA), were packed at 9500 psi using the slurry packing procedure.

The kinetic parameters related to column permeability characteristics were obtained using *n*-hexane/acetonitrile (99/1) as eluent, delivered at a flow rate of 1 mL/min at 20 °C.

The column dead times (t_0) were determined from the elution times of an unretained marker (1,3,5-tri-*tert*-butylbenzene, using dichloromethane/methanol 97/3 as eluent).

Columns efficiency towards achiral solutes (methyl benzoate, acetophenone, nitrobenzene, 1,3-dinitrobenzene) was evaluated using n-hexane/chloroform stabilized with ∼0.25% ethanol (90/10) as eluent, delivered at a flow rate of 1 mL/min at 30 °C. Each injection was repeated at least two times.

Inverse size exclusion chromatography was performed using a total of 17 compounds (polystyrenes 470000-500, *p*-terphenyl, anthracene, biphenyl, naphthalene, toluene) with molecular masses ranging from 470,000 to 92. Individual compounds were injected into each column using THF as eluent, delivered at a flow rate of 1 mL/min at 30 °C. Each injection was repeated at least two times.

Racemic and enantiomerically pure samples were eluted in normal phase (NP) mode using a mobile phase consisting of one or two apolar organic solvents (*n*-hexane, dichloromethane) mixed with one or two polar organic modificators (2-propanol, ethanol, methanol, dioxane, tetrahydrofurane) and in polar organic mode (POM) using a mixture of polar organic solvents (acetonitrile, methanol) buffered with 20 mM ammonium acetate, delivered at a flow rate of 1 mL/min at 25 °C.

All the chromatograms were recorded at the wavelength of 254 nm; for compounds **14**–**16** and **22** a wavelength of 210 nm was used. Chiroptical detection by circular dichroism was used in some instances to check elution order of the enantiomers from the column.

3. Results and discussion

3.1. Synthetic strategy for the preparation of CSP1

In this work, we describe the preparation, characterization and chromatographic applications of a new polymeric chiral stationary phase, CSP1. The results are compared with those obtained on the related CSP2, prepared by the classical solution polymerization approach. In the classical method of radical polymerization for the preparation of polymeric CSPs, the chiral monomer and the radical initiator are both kept in solution and the solid support is usually activated with a polymerizable group, such as a vinyl or acryloyl fragment. With this approach, the chiral polymer is mainly formed in solution, and subsequently, it becomes end-grafted to the support surface. In general, only a reduced amount of polymer can be immobilized following such a *g-to* technique, because the steric constraint generated by the already grafted polymeric fragments inhibits the covalent attachment of additional polymer chains (Fig. 1, top left). Pore occlusion by large polymeric fragments can additionally lead to uneven and incomplete surface coverage. The more successful *g-from* approach is based on immobilized initiators that permit the generation of grafted polymer molecules directly on the surface of mesoporous silica particles. In the ideal case, the *g-from* process is not only *surface-initiated* but is also *surface-confined*, so that polymer growth is not occurring in solution (Fig. 1, bottom left). In the real case, however, the presence of reactive species escaping the surface and the internal volume cannot be completely excluded, and polymerization is no longer

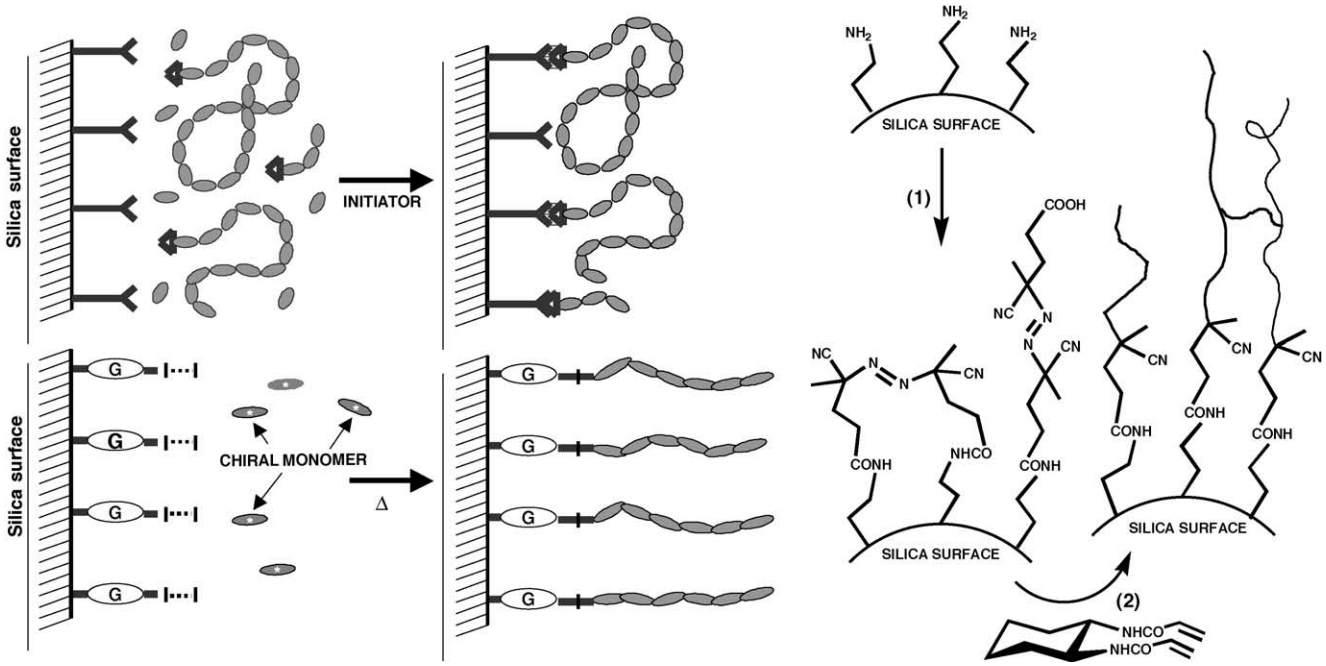

Fig. 1. *g-to* (top left) and *g-from* (bottom left) polymerization approches. Synthetic strategy for the preparation of CSP1 (right). (1) ACPA-dichloride, 1-methoxy-2-methyl-1-(trimethylsyliloxy)-1-propene; anhydrous CH_2Cl_2 or ACPA, EEDQ, DMF. (2) Heat; anhydrous and degassed $CHCl_3$.

surface-confined. Nonetheless, polymer growth from the surface will represent the favored process, and polymeric chains grown in solution, if do not undergo subsequent end-grafting during the reaction period, can be easily removed from the final material.

In our work, we used an azo compound as radical initiator, 4,4′-azobis-4-cyanopentanoic acid (ACPA), that was covalently grafted to the surface of APSG silica though the formation of amide bonds with the aminopropyl groups. The whole process (Fig. 1, right) starts with the silanization of the silica surface with 3-aminopropyltriethoxysilane. The radical initiator, in the activated form of the dichloride of ACPA, is then condensed with the 3-aminopropyl groups using 1-methoxy-2-methyl-1-(trimethylsyliloxy)-1-propene as HCl scavenger. During this step, a concomitant end-capping of the residual free silanols is probably realized by the trimethylchlorosilane released from the scavenger itself.

Alternatively, activation of 3-APSG can be more conveniently obtained in a single step using ACPA and a condensing agent like EEDQ. Amide linkages between the silica aminopropyl groups and the diacid are formed smoothly at room temperature and by-products are easily removed by filtration and exhaustive washing.

The two procedures yield azo-activated silica matrixes that are very similar in their physico-chemical properties and the final CSPs prepared from the two intermediates have almost the same chromatographic behavior. For small-scale preparations, the EEDQ mediated coupling of ACPA to aminopropyl silica is more convenient than the two-step route based on the dichloride of APCA.

The azo-activated silica particles are then heated in the presence of the *N*,*N*′-diacryloyl derivative of (*R*,*R*)-1,2-diaminocyclohexane. Thermal decomposition of surface-tethered APCA initiates the polymerization from the silica surface, yielding the final CSP, containing the covalently grafted chiral polymer in the form of a uniform, thin layer.

3.2. Chemical and physical characterization of azo-activated silica and of CSP1

Chemical characterization of the azo-activated phase and of the final CSP1 was based on results from elemental analysis, diffuse reflectance infrared spectroscopy (DRIFT), and differential scanning calorimetry (DSC).

Information on the composition of the initiator layer of 3-APSG-AZO was gained by combining the results from elemental analysis (Table 1) with those coming from DSC. Data on carbon and nitrogen contents of 3-APSG and 3-APSG-AZO show that all the aminogroups of 3-APSG are

Table 1
Characterization by elemental analysis of CSP1 and CSP2 prepared on Daisogel SP-300-5P Calculations are based on carbon

	3-APSG	3-APSG-AZO	CSP1	VSG	CSP2
Carbon (%)	1.35	3.70	10.36	1.14	6.82
Hydrogen (%)	0.54	0.78	1.68	0.42	1.08
Nitrogen (%)	0.48	1.21	2.19	–	1.13
μmoles g^{-1}	375	279	392	475	401
μmoles m^{-2}	3.37	2.61	4.13	4.24	3.93

The chiral monomer unit is considered as the substrate for the last step.

converted to amide groups in the activation stage, giving a surface density of azo-initiator of 2.61 μmoles m^{-2}, corresponding to 279 μmoles g^{-1} of matrix. Theoretical %C values for the one-to-one and two-to-one reactions between the surface aminogroups and the dichloride of ACPA (i.e. one-end tethering and two-end bridging) are ∼5.5% and ∼2.7%, respectively. The experimental value is found between these two extremes and is consistent with a complete conversion of the aminogroups, about 65% of them having reacted in the bridging mode. The fraction of ACPA groups that is one-end tethered will release, upon thermal activation, a radical fragment that escapes the silica surface. Although these free fragments are no longer *surface-confined*, they are mainly restricted within the micropores of silica particles where the growth of long polymeric chains is prevented by the steric constraints generated by the pores dimension and architecture.

Activation of 3-APSG by the azo initiator is accompanied by small changes in the DRIFT spectra. These changes, however, are diagnostic of the presence of azo and amide groups on the silica surface (weak signal at 2244 cm^{-1}, CN stretching; and signals at 1649 and 1548 cm^{-1}, amide vibrations).

The thermal decomposition behavior of the immobilized azo molecules, as studied by DSC, adds further evidence about the presence of reactive azo fragments on the surface of 3-APSG-AZO and confirms the elemental analysis results about the surface coverage. Thermal decomposition of bulk ACPA, a solid at room temperature, shows a sharp exotherm of decomposition with a peak temperature of 120 °C [16]. Unlike AIBN and other azo initiators, bulk ACPA does not show a melting endotherm. Thus, the DSC results of bulk ACPA and 3-APSG-AZO (Fig. 2) can be directly compared. 3-APSG-AZO shows the azo decomposition peak at 124 °C, thus very close to the value of bulk ACPA. However, the DSC curve of ACPA is very broad, with left and right limits at 82 and 159 °C, respectively. This is probably the result of local, microenvironmental differences experienced by the surface-grafted azo initiator. The DSC curve of 3-APSG-AZO can also be used to extract information on the amount of active azo groups present on the activated silica. Here we assume that the azo thermal decomposition, studied by DSC at a heating rate of 10 °C min^{-1}, occurs in the same way as that of bulk ACPA and is not affected by the immobilization on the silica surface. Accordingly, based on the molar enthalpy of decomposition ΔH_{ACPA} = 160 kJ mol^{-1} of bulk ACPA [16], the amount of immobilized, reactive azo fragments can be calculated from the ratio of the integral of the DSC signal of 3-APSG-AZO (I_{dec} = 44.77 J g^{-1}) and ΔH_{ACPA}. The surface coverage calculated in this way (280 μmoles g^{-1}) is in excellent agreement with that obtained by elemental analysis (279 μmoles g^{-1}).

Data on carbon content for the final CSP1 show an average surface density of monomer units of 4.13 μmoles m^{-2}, corresponding to 392 μmoles of monomer units per gram of matrix. If the chiral polymer were assumed to have a uniform distribution giving a complete coverage of the silica surface, it would be composed by short oligomeric chains, according to the results of elemental analysis. However, steric consideration and the results of ISEC studies (see below) suggest a surface organization characterized by longer polymer chains evenly spaced at lower grafting densities.

In the DRIFT spectrum of CSP1, intense signals arising from the chiral polymer are clearly visible in the amide-stretching region (3078, 1646 and 1542 cm^{-1}) and in the aliphatic stretching and bending regions (2941, 2860, 1451 cm^{-1}). Similar results in terms of surface coverage were obtained for CSP2 (average value of 3.93 μmoles m^{-2}, corresponding to 401 μmoles g^{-1} of matrix).

The DSC trace for CSP1 no longer shows the exothermic transition due to azo decomposition, indicating that a large fraction of the surface-bound initiator molecules were thermally decomposed during the last synthetic step (the detection limit of the DSC measurements can be considered around 30 μmol g^{-1}).

Surface characterization of CSP1 was also carried out using scanning electron microscopy (SEM). Under low

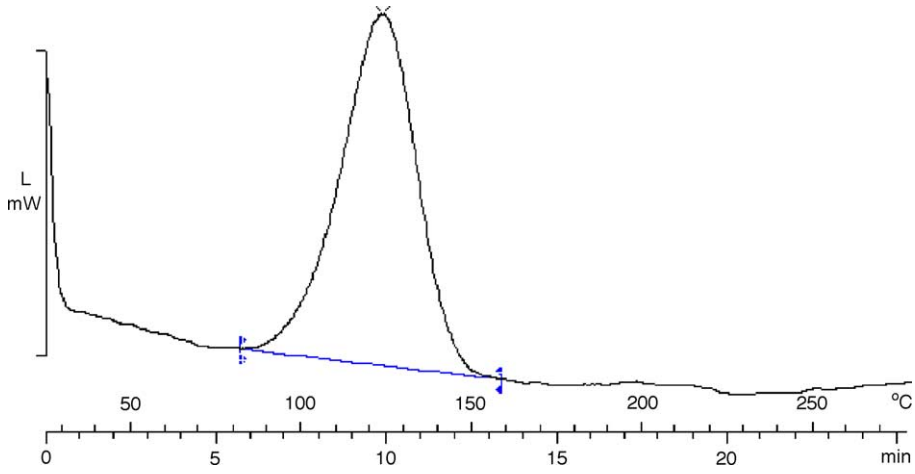

Fig. 2. DSC trace of 3-APSG-AZO. Heating rate = 10 °C min^{-1}.

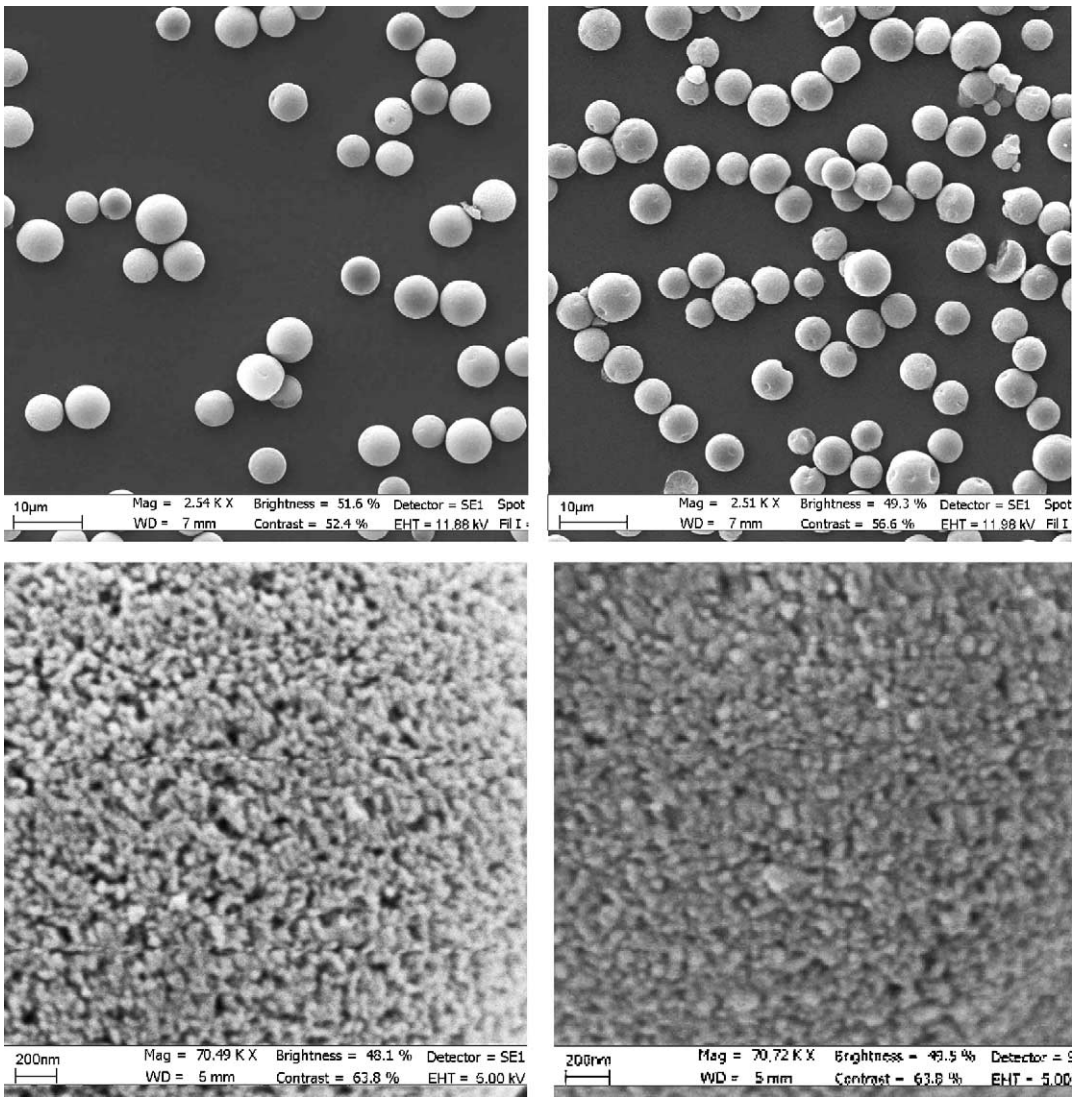

Fig. 3. SEM images of Daisogel SP-300-5P (left) and CSP1 (right). Magnification 2.5×10^3 (top) and 70×10^3 (bottom).

magnification conditions, CSP1 appears as consisting of micron-sized particles with intact spherical shape and with no evident sign of interparticle aggregation. At higher magnifications, details of the pores structure are recognizable (Fig. 3, right). Comparison of SEM images of CSP1 and of Daisogel SP-300-5P, taken under identical conditions, reveals that the pore morphology is not greatly affected by the polymer grafting process (Fig. 3, left). The pore structure is still clearly observable for CSP1, although the average dimensions of the observable holes is substantially reduced compared to the starting silica matrix. This finding is in agreement with ISEC studies (see below).

Additional SEM analyses were carried out on the organic material recovered after HF treatment of CSP1 (Fig. 4). At low magnification, several spheroidal objects with average dimensions of 2 μm are observed, together with some completely collapsed, flat objects of the same dimensions. The spheroids are most likely a negative image of the original internal surface of CSP1, and persistence of the spherical shape is certainly due to partial cross-linking between adjacent polymer chains. Size reduction and collapse of the original microspheres are due to the lack of mechanical strength of the organic material and are the result of the high vacuum treatment of the samples required to obtain the SEM images.

Attempted characterization of the free chiral polymer grown in the absence of a solid support (chloroform solution, AIBN as a radical iniator) was unsuccessful due to the complete insolubility of the polymeric material in all the common solvents.

3.3. ISEC determination of the external and internal porosities of the polymeric stationary phases

The influence of pore-size distribution on a column performance is widely recognized particularly for polymeric stationary phases. Moreover, critically important to the

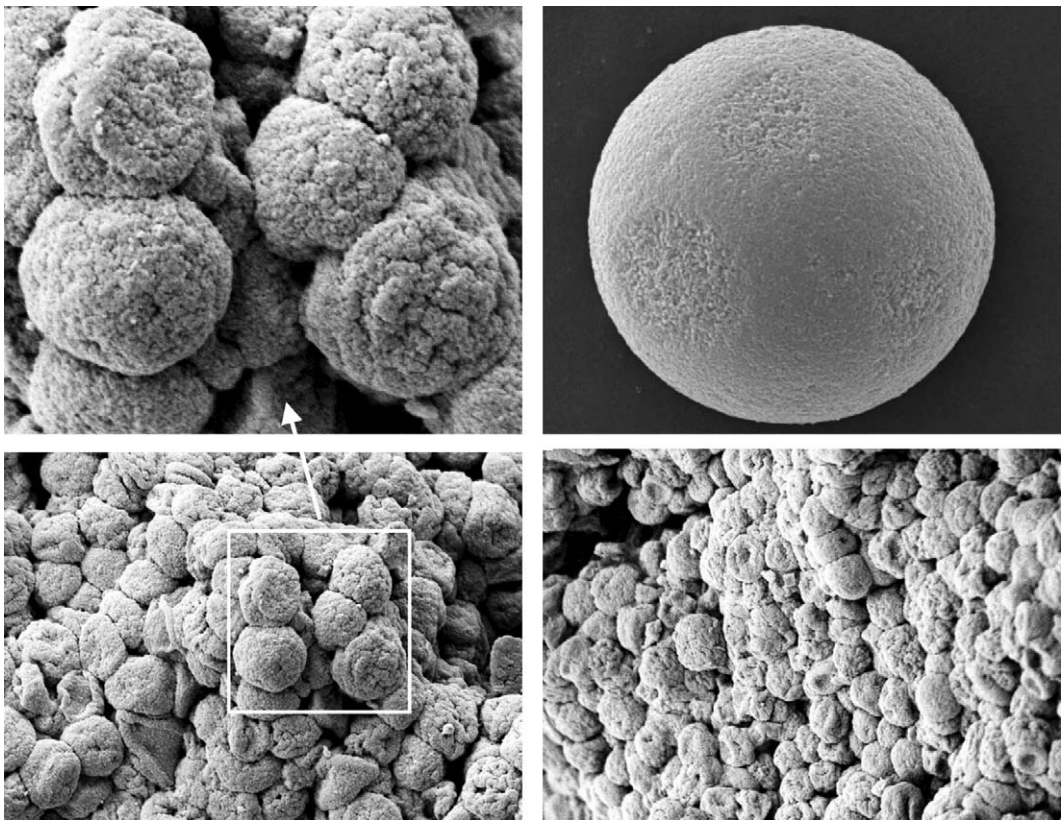

Fig. 4. SEM images of CSP1 before (top right) and after the HF treatment (top left and bottom). Magnifications are 21×10^3 (top), 9×10^3 (bottom left) and 5×10^3 (bottom right).

usefulness of a polymeric stationary phase is the pore accessibility, because a large extent of pore blockage can result in very low chromatographic efficiency. Therefore, it is necessary to determinate the external and internal pore volumes (hence, porosities) of the different packing materials. A very rapid and accurate method for this determination is the inverse size exclusion chromatography (ISEC) technique [17]. The total volume of a liquid chromatographic column (V_k) can be split into three different contributions: the inter-particle or external pore volume (V_e), the internal pore volume (V_i) and the unaccessible volume (V_u), that is the sum of the silica particle volume, the closed pore volume and the volume of the bonded organic layer. ISEC studies were performed on columns packed with CSP1, CSP2 and bare Daisogel- SP-300-5P, using a set of polystyrene standards and aromatic test solutes, and tetrahydrofurane as eluent.

Plots of the logarithm of the molecular masses M_w of the used probes versus their elution volumes are given in Fig. 5 for the three columns. In each plot, two different curves, approximately linear, can be identified in the low to medium elution volume regions. They correspond to the retention contributions of the two different types of pores: those that belongs to the silica particles (internal pores, the sum of their volumes is the internal volume V_i) and those located between the particles (external pores, the sum of their volumes is the external volume V_e). The coordinates of the intercept of the two regression lines for each plot give the value of the external volume (V_e) and the corresponding exclusion pore size Φ_e. An estimate of the different Φ_e values can be obtained using the formula $\Phi_e = 0.246\ (M_w)^{0.588}$ [18], where M_w is the molecular weight corresponding to the intersection points and Φ_e values are given in angstrom (Table 2). It is seen that the value of exclusion pore size Φ_e for the starting silica $\Phi_e = 347$ Å is in good agreement with the expected value of 300 Å given by the manufacturer. The same parameter is reduced to one third for both CSP1 and CSP2, indicating that their average

Table 2
Comparison of internal and external porosities obtained on Daisogel SP-300-5P, CSP1 and CSP2

Column packed with	V_T (mL)	V_e (mL)	V_i (mL)	Φ_e (Å)	ε_T	ε_e	ε_i
Daisogel SP-300-5P	3.22	1.57	1.65	347	0.78	0.38	0.64
CSP1	2.83	1.62	1.21	106	0.68	0.39	0.48
CSP2	2.85	1.42	1.43	102	0.69	0.34	0.53

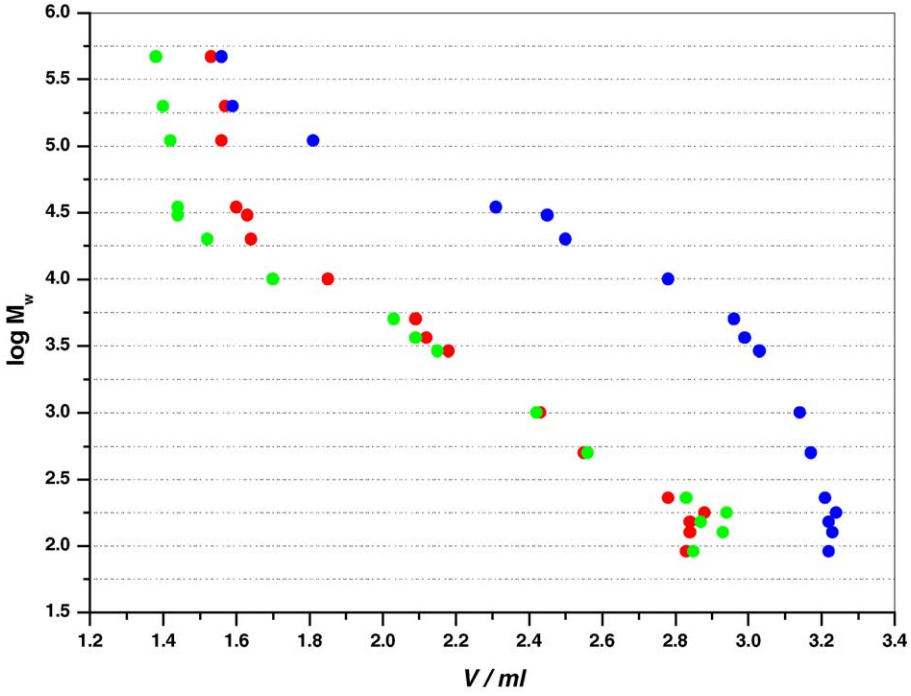

Fig. 5. Graphical representation of log M_w vs. retention volume for 17 compounds (polystyrenes 470000-500, *p*-terphenyl, anthracene, biphenyl, naphthalene, toluene). Eluent, THF; flow rate, 1 mL/min; temperature, 30 °C; detector, UV at 254 nm (●) Daisogel SP-300-5P; (●) CSP1; (●) CSP2).

pore dimensions are reduced to about 100 Å after the polymerization step.

The volume fraction of the external pores, or external porosity ε_e, corresponding to the retention volume V_e, and the total pore volume fraction or total porosity ε_T, corresponding to the retention volume of toluene V_T, are defined by:

$$\varepsilon_e = \frac{V_e}{V_k} \qquad \varepsilon_e = \frac{V_e}{V_k}$$

where V_k is the total column volume geometrically calculated.

From the total balance of porosity, it is possible to calculate ε_i (the internal porosity, related to the volume of the internal pores V_i):

$$\varepsilon_T = \varepsilon_i(1 - \varepsilon_e) + \varepsilon_e$$

In Table 2, are shown the results obtained for the three columns packed with CSP1, CSP2 and Daisogel SP-300-5P.

As expected, the total porosity ε_T, corresponding to the total volume V_T, is greater for the non derivatized chromatographic support, due to a higher value of internal porosity ε_i. CSP1 maintains almost the same external porosity ε_e and retention volume V_e as for Daisogel SP-300-5P, while its internal porosity ε_i shows a substantial reduction. This means that the chiral polyamide polymer of CSP1 is nearly all grafted within the porosities. Conversely, CSP2 exhibits the lowest value of external porosity ε_e and retention volume V_e; this is most likely associated to a large extent of extra pores growth of the polymer chains during classical polymerization.

3.4. Study of the permeability characteristics of the polymeric stationary phases

The influence of the starting silica material on column permeability was carefully evaluated for the chiral polymeric materials prepared on Daisogel SP-300-5P, Kromasil Si-200 and Kromasil Si-100 silica gel, having an average pore diameters of 300, 200 and 100 Å, respectively. The flow resistance (Φ) and the permeability (K_0) parameters [19] were chosen as principal parameters reflecting the polymerization outcome in terms of layer thickness, uniform coverage, and pores occlusion.

The optimum values of the flow resistance ($\Phi = 602$) and permeability ($K_0 = 4.15 \times 10^{-14}$ m^2) were obtained in the case of CSP1 prepared on Daisogel SP-300-5P. Good results were reached using Kromasil Si-200 ($\Phi = 635$, $K_0 = 3.94 \times 10^{-14}$ m^2). Nevertheless, a further reduction in the pore diameter (Kromasil Si-100) caused a considerable rising of Φ (777) and lowering of K_0 (3.22×10^{-14} m^2). This behavior may be due to partial pore blockage as the polymer chains grow inside very small porosities. Permeability studies carried out on CSP2 (prepared using Daisogel SP-300-5P) show values of Φ (699) and K_0 (3.57×10^{-14} m^2) that are also indicative of poor permeability performances. This finding suggests that the classical polymerization process (*g-to*) may alter the internal pore structure, an indication in agreement with the results obtained by ISEC.

The overall picture emerging from the combined SEM analysis of CSP1 and of HF treated CSP1, elemental analysis, ISEC and Van Deemter analysis of CSP1 and CSP2

is that of a polymer structure in CSP1 consisting of evenly distributed, ordered chains that results in favorable analyte mass transfer kinetics. The average pore dimensions of about 100 A derived from ISEC studies, combined with elemental analysis data, is consistent with the presence on CSP1 of linear polymeric chains originating from a fraction of the surface-linked azo initiators. Inspection of SEM images of CSP1 after HF treatment suggests that the polymer chains are cross-linked on the original material.

3.5. *Efficiency characterization of columns packed with CSP1, CSP2 and Daisogel SP-300-5P*

Various phenomena lead to band broadening in liquid chromatography. The major contributions are attributed to columnar effects and can be related to the quality of column packing, longitudinal diffusion and resistance to mass transfer between mobile and stationary phases [20].

The chromatographic performances of CSP1 were evaluated in a series of flow studies and compared to those obtained on the columns packed with CSP2 and Daisogel SP-300-5P. Van Deemter plots for a series of achiral aromatic compounds (methyl benzoate, acetophenone, nitrobenzene, 1,3-dinitrobenzene) are shown in Fig. 6 for the three columns packed with CSPs 1 and 2 and with bare silica Daisogel SP-300-5P. The columns packed with CSP1 and with Daisogel SP-300-5P show good to excellent efficiency values, with the minima of the curves observed at flow rates between 0.5 and 1.0 mL/min. Reduced plate height values at the minima of the curves are in the range 3.5–3.8. As the flow rate is increased, the column packed with CSP1 shows a more rapid worsening of the efficiency compared to the silica column, as expected on the basis of the polymeric nature of the bonded selector of CSP1. The column packed with CSP2 shows poor overall kinetic performances, as evidenced by the Van Deemter plots shown in Fig. 6. While the reduced efficiency of the column, containing CSP2 is largely due to a more difficult packing procedure (large A term of the Van Deemter equation), the higher slope of the high-flow rates portion of the plots (C term) is clearly indicative of poor mass transfer in the stationary zone of CSP2. This could either be due to small pore blockage or to an inhomogeneous distribution of the polymer layer.

3.6. *Enantioresolution capabilities of CSP1*

A large set of chemically diverse chiral solutes was used to evaluates the enantioselectivity of CSP1 (Figs. 7 and 8). The screening set includes both neutral and ionizable compounds that were separated using several mobile phase compositions ranging from typical normal phase eluents (hexane and polar modifier, dichloromethane and polar modifier) to polar organic or polar ionic eluents (acetonitrile/methanol mixtures plus ammonium acetate). The results of screening CSP1 under normal phase conditions are gathered in Table 3. Several compounds are resolved with enantioselectivity values

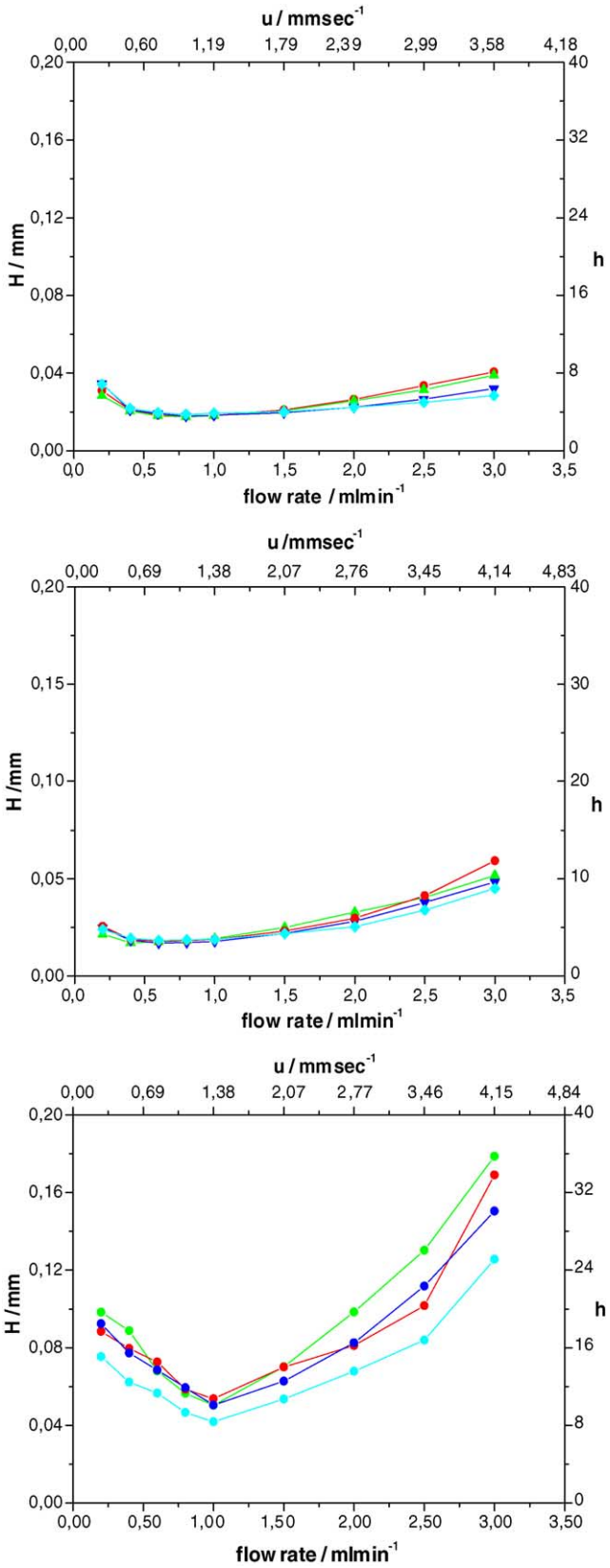

Fig. 6. Flow-curve comparison of columns packed with bare silica (top), CSP1 (middle) and CSP2 (bottom). Solutes: (▲) methyl benzoate; (▼) acetophenone; (●) nitrobenzene; (■) 1,3-dinitrobenzene.

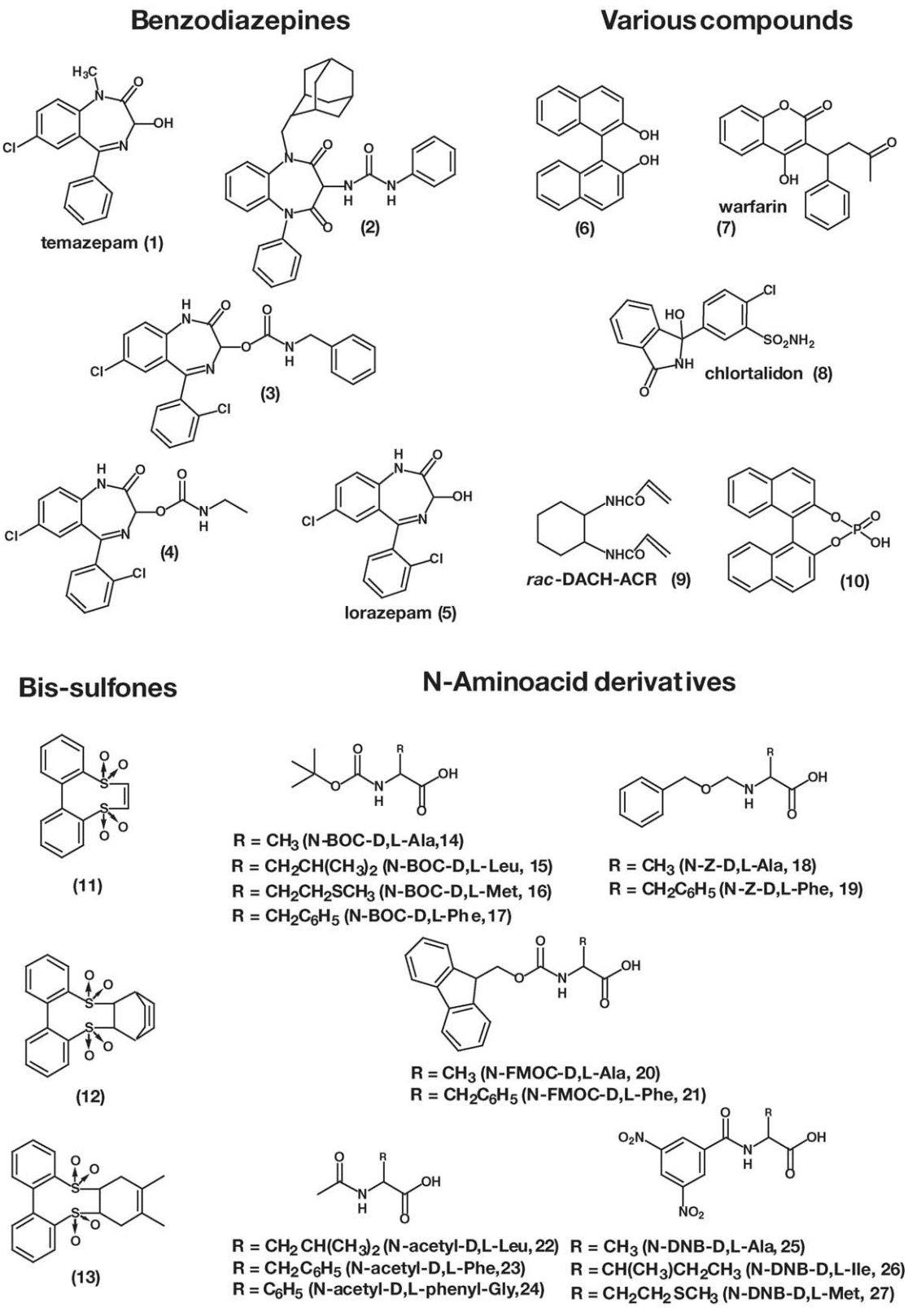

Fig. 7. Structures of chiral compounds resolved by HPLC on CSP1.

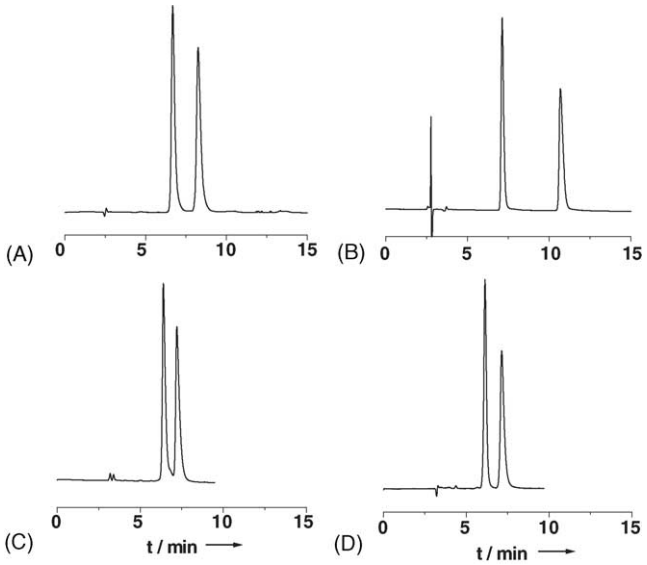

Fig. 8. Some examples of chromatographic resolution on CSP1; for chromatographic conditions and parameters, see Tables 3 and 4 (A, compound **1**, eluent b; B, compound **6**, eluent a; C, compound **8**, eluent f; D, compound **21**, eluent f).

(α in Table 3) exceeding 2, leading to large resolutions in short analysis time. Some general trends of enantioselectivity as a function of the analyte structure are apparent from the data collected. Retention of the enantiomers of the structurally related 3-hydroxy-benzodiazepin-2-ones (compounds **1**, **3**–**5**;

Table 3
Chromatographic parameters obtained in normal phase (NP) mode for compounds **1**–**7** and **11**–**13** resolved on CSP1

Compounds	k_1	α	R_s	Eluent
1	0.13	1.58	0.48	a
	1.48	1.39	3.84	b
	2.45	1.56	5.82	c
	4.51	1.71	6.34	d
2	0.38	1.60	3.08	a
	1.18	1.29	2.04	b
3	1.44	4.29	19.63	a
	1.84	2.38	7.43	b
4	1.51	3.89	18.15	a
	1.34	2.33	5.96	b
5	5.64	2.06	11.17	a
	5.65	1.55	3.68	b
6	1.74	1.90	11.12	a
	2.73	1.40	4.25	b
	4.65	1.47	4.79	d
7	3.15	1.14	1.21	c
11	4.54	1.10	2.42	e
12	2.81	1.09	1.56	e
13	2.03	1.08	1.31	e

Eluents: (a) dichloromethane/methanol (97/3); (b) *n*-hexane/ethanol (50/50); (c) *n*-hexane/1,4-dioxane/methanol (60/39/1); (d) *n*-hexane/tetrahydrofuran/methanol (50/49/1); (e) *n*-hexane/dichloromethane/methanol (80/20/0.5). Flow rate, 1 mL/min; temperature, 25 °C; detector, UV at 254 nm.

Table 4
Chromatografic parameters obtained in polar organic mode (POM) for compounds **5**–**6** and **14**–**21** resolved on CSP1

Compounds	k_1	α	R_s	Eluent
5	1.07	1.74	5.98	f
	2.05	1.94	6.44	g
6	0.52	1.17	1.31	f
	0.88	1.26	2.50	g
8	1.13	1.24	2.02	f
	3.13	1.32	2.36	g
9	0.38	1.81	3.27	I
10	1.28	1.33	2.63	f
14	1.34	1.14	1.46	h
15	1.16	1.33	2.82	h
16	1.27	1.36	3.09	h
17	1.29	1.24	2.53	h
18	1.79	1.21	1.64	h
19	1.67	1.26	2.43	h
20	1.06	1.23	2.02	f
21	1.04	1.32	2.72	f
22	0.97	1.28	1.85	f
23	1.02	1.16	1.40	f
24	1.59	1.14	0.91	f
25	0.97	1.18	1.25	f
26	0.76	1.40	2.30	f
27	0.94	1.30	1.64	f

Eluents: (f) acetonitrile/methanol (70/30) 20 mM ammonium acetate; (g) acetonitrile/methanol (85/15); (h) acetonitrile/methanol (85/15) 20 mM ammonium acetate; (i) acetonitrile/methanol (95/5) 20 mM ammonium acetate. Flow rate, 1 mL/min; temperature, 25 °C; detector, UV at 254 nm (210 nm for compounds **14**–**16** and **22**).

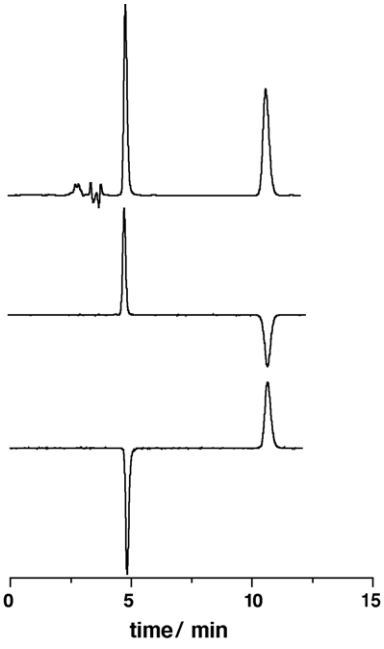

Fig. 9. Resolution of *rac*-**3** on columns packed with enantiomeric versions of CSP1. Eluent, dichloromethane/methanol 95/5; flow rate, 1.0 mL/min; $T = 25$ °C; detections, UV and CD at 254 nm. (Top and middle) CSP1 from (*S*,*S*)-DACH-ACR; (bottom) CSP1 from (*R*,*R*)-DACH-ACR.

eluent a) is greatly affected by the presence of H-bonding sites in the analytes: compound **5**, having both the amidic NH and the alcoholic OH available to complementary H-bonding sites on the CSP shows the highest retention, while N1 methylated **1** and carbamate derivatives **3** and **4** are less retained. A free NH at position 1 seems to be required for high enantioselectivities (compound **1** versus **5**), while conversion of the free OH in position 3 to a carbamate greatly increases enantioselectivity (compounds **5** versus **3** and **4**). Chromatograms showing the enantioresolution of compound **3** on two columns, containing CSP1 prepared from either (*R*,*R*) or (*S*,*S*)-DACH are shown in Fig. 9. Dual detections by UV and circular dichroism (CD) clearly show elution order inversion and a complete chemical equivalence of the two enantiomeric stationary phases. Additional retention and enantioselectivity data presented in Table 3 clearly show the effect of H-bonding on solute-stationary phase interaction and recognition. It is noteworthy that in most cases the highest enantioselectivity values are obtained using mobile phases that have good analyte solvating properties. This point has practical relevance for enantioseparations at preparative levels, where sample solubility in the mobile phase is a prerequisite for a successful resolution. A preliminary loading study was performed on the analytical column packed with CSP1, using compound **6** as a test solute. Solubility of **6** in dichloromethane/methanol 97/3 (eluent a) is high enough to allow a mass overload and to avoid a volume overload of the analytical column. The results of the study (Fig. 10) point to a remarkable loading of 20 mg of **6**.

With polar organic eluents, several strongly polar or acidic compounds are well resolved on CSP1 (Table 4). Interestingly, some of these analytes (compounds **9**, **14**–**17**, **22**) have no aromatic fragment in their structure, indicating that this structural feature is not essential for the enantioselectivity.

Under identical experimental conditions, CSP2 shows slightly lower retention and enantioselectivity values than CSP1. Resolution values (R_s) are significantly lower on CSP2 as a result of its poor kinetic performances.

Fig. 10. Loading study of a 250 mm × 4.6 mm column packed with CSP1. Amount injected in mg, from bottom to top: 0.001, 1, 2, 4, 10, 20 of *rac*-**6** dissolved in the mobile phase at a concentration of 100 mg/mL (bottom trace: 1.0 mg/mL). Eluent, dichloromethane/methanol 97/3; flow rate, 1.0 mL/min; $T = 25\,^{\circ}C$; detections, UV at 350 nm.

4. Conclusions

The surface-initiated polymerization of chiral, enantiopure diacryloyl derivative of *trans*-1,2-diaminocyclohexane on mesoporous azo-activated silica yields a hybrid polymeric stationary phase. The available structural and chromatographic data are consistent with an ordered polymeric layer architecture that yields higher chromatographic performances compared to the analog stationary phase prepared by the alternative procedure using solution initiated polymerization. The new chiral packing material has broad applicability, high enantioselectivity, chemical and thermal inertness and is available in both the enantiomeric forms. At the same time, analytical columns packed with the new material show high overall chromatographic efficiency and high loading capabilities, leading to complete resolutions in short analysis time.

Acknowledgments

Support of this research by Grants from MIUR-PRIN (contract no. 2003039537) and Istituto Pasteur-Fondazione Cenci Bolognetti of University “La Sapienza” of Rome” is gratefully acknowledged.

References

[1] G. Subramanian, Chiral Separation Techniques: A Practical Approach, second ed., Wiley-VCH, Weinheim, 2001.
[2] T.E. Beesley, R.P.W. Scott (Eds.), Chiral Chromatography, John Wiley and Sons Ltd., Chichester, 1998.
[3] S. Ahuja, Chiral Separations: Applications and Technology, American Chemical Society, Washington, DC, 1996.
[4] F. Gasparrini, D. Misiti, C. Villani, J. Chromatogr. A 906 (2001) 35.
[5] J. Haginaka, J. Chromatogr. A 906 (2001) 253.

[6] E. Yashima, J. Chromatogr. A 906 (2001) 105.
[7] C. Yamamoto, Y. Okamoto, Bull. Chem. Soc. Jpn. 77 (2004) 227.
[8] C. Perrin, V.A. Vu, N. Matthijs, M. Maftouh, D.L. Massart, Y. Vander Heyden, J. Chromatogr. A 947 (2002) 69.
[9] S. Edmondson, V.L. Osborne, W.T.S. Huck, Chem. Soc. Rev. 33 (2004) 14.
[10] O. Prucker, J. Ruhe, Macromolecules 31 (1998) 592.
[11] X. Huang, M.J. Wirth, Anal. Chem. 69 (1997) 4577.
[12] J. Parvole, L. Billon, J.P. Montfort, Polym. Int. 51 (2002) 1111.
[13] H. Kanazawa, T. Sunamoto, E. Ayano, Y. Matsushima, A. Kikuchi, T. Okano, Anal. Sci. 18 (2002) 45.
[14] F. Gasparrini, D. Misiti, C. Villani. PCT Int. Appl. (2003) 25 pp. CODEN: PIXXD2 WO 2003079002. Columns packed with CSPs prepared in this way (P-CAP) are commercially available from Astec, Whippany, NJ, USA.
[15] B. Galli, F. Gasparrini, D. Misiti, M. Pierini, C. Villani, M. Bronzetti, Chirality 4 (1992) 384.
[16] T. Cheikhalard, L. Tighzert, J.P. Pascault, Angew. Makromol. Chem. 256 (1998) 49.
[17] I. Halasz, K. Martin, Angew. Chem. (Int. Engl.) 17 (1978) 901.
[18] M. Ousalem, X.X. Zhu, J. Hradil, J. Chromatogr. A 903 (2000) 13.
[19] J.H. Knox, H.P. Scott, J. Chromatogr. 282 (1983) 297.
[20] R.L. Hansen, J.M. Harris, Anal. Chem. 67 (1995) 492.